Colloid & Polymer Science Colloid Polym Sci 272:1420–1429 (1994)

Molecular dynamics of cyclic and linear poly(dimethylsiloxanes)*)

K.U. Kirst, F. Kremer, T. Pakula[1]), and J. Hollingshurst[2])

Institut für Physik, Universität Leipzig, Leipzig, FRG
[1]) Max-Planck-Institut für Polymerforschung, Mainz, FRG
[2]) Dept. of Chemistry, University of York, Heslington, York UK

*) *Dedicated to Prof. E.W. Fischer on the occasion of his 65th birthday.*
"*Fast macht' das WLF ihn krank, jetzt raucht er wieder, Gott sei Dank!*" (*frei nach Wilhelm Busch*)

Abstract: Dielectric spectroscopy (10^{-1} Hz to 10^{7} Hz) has been employed to study the molecular dynamics of a series of cyclic and linear polydimethylsiloxanes (PDMS) of various molecular weights ranging from 300 to 10000 g/mol in the temperature range above the glass transition (from 130 K to 190 K). The observed α-relaxation depends strongly on both molecular weight and structure of the samples. For linear PDMS oligomers, the α-relaxation shifts towards lower temperatures with decreasing molecular weight in good accordance with the Fox–Flory-model. Cyclic PDMS reveals a qualitatively different molecular weight dependence: for a given temperature the α-relaxation time increases with decreasing ring length, but has a maximum for small oligomers (degree of polymerization $n \approx 6$). The shape of relaxation curves and, with it, the relaxation time distribution is independent from length and architecture of the chains. The observed experimental findings are in qualitative agreement with dynamic Monte-Carlo simulations.

Key words: Dielectric spectroscopy – molecular dynamics – polydimethylsiloxane – cyclic polymers – glas transition – dynamic Monte–Carlo simulation

1. Introduction

The effect of a linear or ring-shaped architecture of polymers on their molecular dynamics has been studied both experimentally [1, 2, 9, 10, 11, 6] and theoretically [7, 8]. For linear polymers, Fox and Flory found a linear relationship between the glass transition temperature and the inverse molecular mass [1]. The opposite trend was observed for cyclic polymers [2]. Differences due to topology arise from three facts: i) the mobility of end-groups in linear chains, ii) frustration of segmental rotational diffusion in small rings, and most important iii) the much smaller configurational entropy of cyclic chains compared to that of linear molecules.

Besides viscosity [9], diffusion coefficient [10], and glass transition temperature [2, 11, 12], the dielectric relaxation reveals information about molecular dynamics. Especially, dielectric spectroscopy supplies this information over a broad frequency- and temperature range. In the present work, it is employed to study the α-relaxation (dynamic glass transition) of linear and cyclic PDMS. PDMS was chosen as a well known polymeric system with segmental dipole moments perpendicular to the chain contour.

The results are compared with dynamic Monte–Carlo simulations based on the cooperative motion algorithm [13].

2. Experimental

2.1 Preparation of the samples

Fractions of linear Poly(dimethylsiloxanes) $(CH_3)_3SiO[(CH_3)_2SiO]_nSi(CH_3)_3$ and the cyclic

Table 1. Characterization of the samples and the Havriliak–Negami-fit parameters of the α-relaxation for linear and cyclic PDMS-chains, respectively. $\bar{n}$ is the average number of repeat units, $\bar{M}_n$ the number average molecular weight and M_w/M_n the polydispersity. The value of $\Delta\varepsilon$ is extrapolated from the measured spectra to a temperature of 298 K. For the fit-parameters α and γ the temperature dependence is negligible.

Sample	Number of bonds	$\bar{n}$	$\bar{M}_n$ (g/mol)	$\frac{M_w}{M_n}$	$\Delta\varepsilon$	α	γ
LIN08	8	3	310	1.00	0.442	0.89	0.47
LIN11	11	4.5	420	1.02	0.516	0.86	0.47
LIN17	17	7.5	640	1.01	0.565	0.86	0.47
LIN20	20	9	750	1.02	0.573	0.86	0.47
LIN22	22	10	830	1.01	0.569	0.87	0.47
LIN24	24	11	900	1.02	0.579	0.87	0.48
LIN30	30	14	1120	1.02	0.571	0.86	0.47
LIN56	56	27	2080	1.03	0.622	0.86	0.47
LIN57	57	27.5	2120	1.05	0.636	0.86	0.47
LIN86	86	42.5	3230	1.11	0.622	0.86	0.47
LIN112	112	55	4160	1.15	0.633	0.86	0.47
LIN187	187	92.5	6930	1.17	0.640	0.86	0.47
LIN280	280	139	10370	1.15	0.633	0.83	0.49
CYC08	8	4	296	1.00	–	–	–
CYC11	11	5.5	410	1.03	0.369	0.86	0.47
CYC12	12	6	440	1.03	0.366	0.86	0.47
CYC14	14	7	520	1.03	0.450	0.87	0.44
CYC22	22	11	810	1.05	0.523	0.88	0.45
CYC30	30	15	1110	1.02	0.529	0.87	0.47
CYC33	33	16.5	1220	1.03	0.553	0.88	0.45
CYC57	56	28	2070	1.04	0.662	0.86	0.47
CYC72	72	36	2660	1.05	0.646	0.86	0.48
CYC114	114	57	4220	1.03	0.642	0.85	0.45
CYC115	115	57.5	4250	1.05	0.628	0.86	0.47
CYC187	187	93.5	6920	1.04	0.610	0.86	0.47

chains ($[CH_3)_2SiO]_n$) were obtained by methods described previously [14, 15]. The linear trimethyl-terminated fractions resulted from preparative GPC starting from Dow Corning dimethicones. The cyclic fractions were recovered from ring-chain equilibrates in toluene at 383 K before being separated into fractions by preparative GPC. Number-average molar masses M_n, heterogeneity M_w/M_n, number of skeletal bonds and of repeat units, x and $\bar{n}$, respectively, and the glass temperatures (determined by DSC) are listed for all samples in Table 1.

In the temperature range corresponding to the dynamic regime of the dielectric measurement systems (10^{-2} Hz–10^{-9} Hz), the stable phase of PDMS is semicrystalline. In order to observe the α-relaxation of the amorphous melt the samples were quenched in liquid nitrogen at a cooling rate faster than 60 K/min in advance of the dielectric experiments. This has been proven to be sufficient to prevent crystallization during the cooling process [2, 16, 17]. Being quenched, the samples were reheated stepwise to the desired measuring temperatures. After an equilibration time of 30 min the dielectric spectra were taken. PDMS tends to crystallize rapidly (both linear and cyclic samples) when reheated above T_g (cold crystallization). During crystallization the α-relaxation, which is assigned to the amorphous bulk PDMS, is replaced subsequently by the slower and weaker α_{cc}-relaxation. When this crystallization was completed (which can be monitored by the vanishing of the α-relaxation in the dielectric spectra), the samples was remelted at ambient temperature and the experiment was continued after another quench.

2.2 Dielectric measurement systems

The dielectric measurements in the frequency range from 10^{-2} Hz to 10^{7} Hz were carried out by a Solartron-Schlumberger frequency response analyzer FRA 1260 supplemented by a high-impedance preamplifier of variable gain and by a Hewlett-Packard 4291, both of them measuring the complex impedance of a sample-filled capacitor [18]. The relative accuracy of the measurement systems for samples having a dielectric loss of 10^{-2} is $\pm 1\%$ in ε' and $\pm 3\%$ in ε''. The fluid siloxanes were given between two gold-plated brass plates (diameter 40 mm and 20 mm, respectively). A sample thickness of 50 μm determined with an accuracy of ± 2 μm was maintained by use of glass-fiber spacers. Taking into account the errors in determination of the sample thickness and errors in the dielectric measuring system, the error of the absolute value of the dielectric data is estimated to be less than 7%.

To describe quantitatively the dielectric spectra the relaxation function of Havriliak Negami [19, 20] (HN) is used:

$$\varepsilon = \varepsilon_\infty + \frac{\varepsilon_{st} - \varepsilon_\infty}{(1 + (i\omega\tau)^\alpha)^\gamma} \,. \tag{2.1}$$

In this notation ε_∞ describes the real part of the dielectric function at $\omega\tau \gg 1$ and ε_{st} the corresponding value for $\omega\tau \ll 1$. The dielectric strength $\Delta\varepsilon$ is defined by $\Delta\varepsilon = \varepsilon_{st} - \varepsilon_\infty$. α characterizes the logarithmic slope of the low-frequency wing and the product $\alpha \cdot \gamma$ that on the high-frequency side. τ is the characteristic relaxation time. The frequency at maximum loss is denoted by f_{max}.

The dielectric relaxation strength is related to the dipole moment via the Kirkwood–Fröhlich equation [27, 28], which can be approximated by

$$\Delta\varepsilon \propto g \cdot n_d \cdot \mu^2 \,, \tag{2.2}$$

with n_d being the number density of dipoles and the Kirkwood–Fröhlich correlation factor $g = 1 + \langle \cos \theta_{i,j} \rangle$. $\theta_{i,j}$ denotes the angle of the i-th dipole to the j-th dipole in its neighbourhood. A strong destructive correlation between dipoles ($\langle \cos \theta_{i,j} \rangle = -1$, i.e. $g = 0$) causes dielectric inactivity.

A conductivity contribution was observed at frequencies below 10^4 Hz. It can be described by the power law

$$\varepsilon'' = \frac{\sigma_0}{\varepsilon_0} \cdot \omega^{s-1} \,, \tag{2.3}$$

where σ_0 is the static conductivity of the sample, ε_0 denotes the permittivity of free space and s is a fitting parameters [21]. From the fitted parameters (τ, α and γ) the mean logarithmic relaxation times as well as the maximum frequencies and the widths of the single relaxation processes were calculated.

The temperature dependence of relaxation processes which are related to the glass transition is generally accepted to be well describable by the Williams–Landel–Ferry (WLF) equation [22] within the region $T_g < T < T_g + 100$ K [23]. With $f = \frac{1}{2\pi\tau}$, this is written as

$$\log \frac{f(T)}{f(T_s)} = \frac{C_1 \cdot (T - T_s)}{C_2 + T - T_s} \,, \tag{2.4}$$

where T_s can be a reference temperature like $T_{g,\mathrm{DSC}}$. On the other hand, it can be defined by a reference relaxation frequency. In this paper it is defined by the relaxation $\omega(T_s) = 2\pi f = 1$ Hz. This temperature can be determined by interpolation of relaxation time vs. temperature curves over a whole series of dielectric experiments, a method by which errors can be minimized. Usually, this dielectrically determined T_s differs by a few degrees from the calorimetric T_g.

3. Experimental results and discussion

Dielectric spectra of amorphous PDMS at temperatures some degrees Kelvin above the calorimetric glass transition show the α-relaxation as plotted in Fig. 1 for the sample LIN24. In this temperature range the stable phase of PDMS is semicrystalline, and the quenched amorphous PDMS undergoes a cold crystallization process when reheated from the glassy state [16, 24, 25, 26]. In consequence, a continuous decrease in dielectric strength of the α-relaxation can be seen in the spectra above a temperature of 158 K given in Fig. 1. The decrease of the α-relaxation, which leads to its complete vanishing, is accompanied by the growth of a second slower relaxation [24], called α_{cc}-relaxation, the strength of which is much smaller than that of the α-relaxation. It

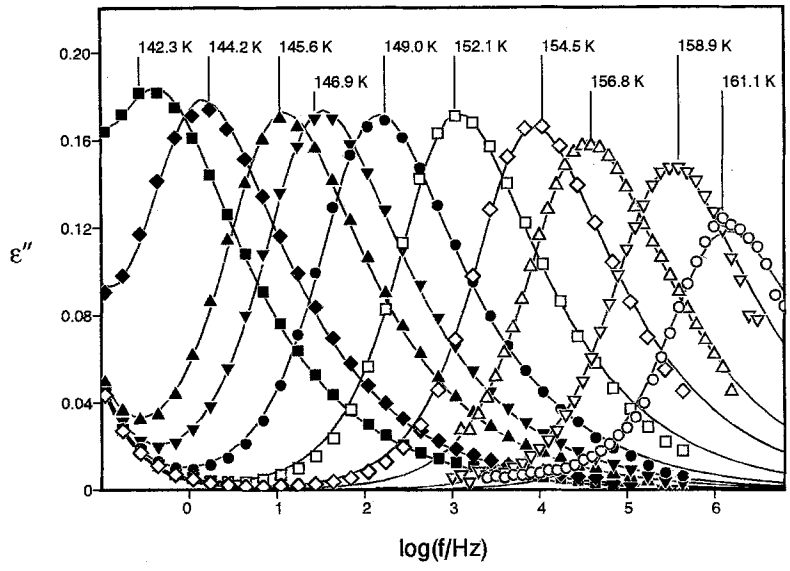

Fig. 1. Dielectric spectra for the sample LIN24 at temperatures in the range from 142 K to 161 K. The lines represent HN-fit curves

corresponds to fluctuations in the remaining amorphous regions of the semicrystalline polymer. These relaxations are assigned to identical dipole moments. For the comparative discussion of the dynamic glass transition in linear and cyclic PDMS the α_{cc}-relaxation is of no relevance.

The dielectric spectra are well describable by Havriliak–Negami-fits. The exponents α and γ are temperature-independent in the observed temperature range. For different samples (see Table 1) their variations are small and cannot be considered significantly correlated, neither to weight not structure of the molecules. This implies an identical relaxation time distribution for all samples. In contrast the relaxation strength $\Delta\varepsilon$ (extrapolated to the value at 298 K) shows a distinct dependence on both features (Fig. 2): For the wider rings, $\Delta\varepsilon_{cyc}(n)$ joins the asymptotic values of $\Delta\varepsilon_{lin}(n)$, but the decrease towards smaller molecular weights is much more pronounced than with linear chains. It leads to complete dielectric inactivity of the α-relaxation for the smallest rings of this study (CYC8).

For linear oligomers, the number density n_d decreases parallel to the molecular weight of the chains. This can be explained by an increase of the volume fraction and number density n_d of end groups, the dipole moments of which are negligible, and a decrease of the number density of polar segments with decreasing chain length. This observation is opposite to results of

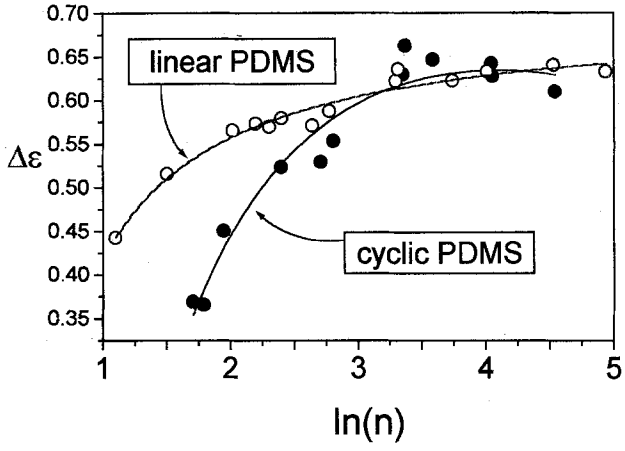

Fig. 2. The dielectric relaxation strength $\Delta\varepsilon$ for linear (open symbols) and cyclic PDMS (solid symbols) vs. natural logarithm of the degree of polymerization. Since the relaxations are observed at different temperatures, for the sake of comparability, the plotted values are extrapolated for a temperature of 300 K by the relation $\Delta\varepsilon \propto \frac{1}{kT}$

Ikada et al. [29] on low-molecular-weight propylene glycols. This contrast is due to the fact that with propylene glycol oligomers $HO{-}[CH(CH_3)CH_2O]_n{-}H$ the terminal OH-groups, the number density of which increases with decreasing molecular weight, are strong dipoles. Thus, the number density development of end groups has the opposite effect for the relaxation strength.

For cyclic chains, the decrease of relaxation strength with decreasing molecular weight can be assigned to a partial neutralization of dipole moments around the rings, or it can be discussed in terms of the Kirkwood–Fröhlich correlation factor. The latter is reduced, because the correlation of segmental dipoles of one ring becomes destructive and segmental librations become increasingly restricted. For a ring of four segments the dipole vectors are assumed to be arranged in the plane of the ring cancelling each other in pairs. This effect was detected by Beevers et al. [30] as a vanishing of the medium square dipole moment $\langle \mu^2 \rangle$ for small rings. The effect of molecular mass and structure on the temperature dependence of the relaxation times is given in activation-plots (Figs. 3 and 4 for linear and ringshaped chains, respectively). In both cases the WLF-curves for samples of different chain length spread out like a fan. At high frequencies they seem to joint to a common asymptotic high-temperature behavior (revealing the local dynamics without cooperative effects), while at lower frequencies the curves are drawn as under due to the different glass transition temperatures of the samples. With linear chains the relaxation rate $1/\tau_{HN}$ for a given temperature increases with decreasing chain length, or vice versa, shorter chains show relaxation of a given rate at lower temperatures. For longer chains a convergence even at low frequencies is observed. In contrast, for cyclic chains the spreading of the activation curves has an opposite molecular weight dependence.

All activation curves can be fitted properly by WLF-functions. The temperature T_s, an originally arbitrary temperature, which often is chosen as a reference temperature identical to the calorimetric glass transition temperature $T_{g,DSC}$, is determined in this analysis by the condition $T_s = T(\tau_{HN} = 1\ s)$. For PDMS this temperature T_s is close to

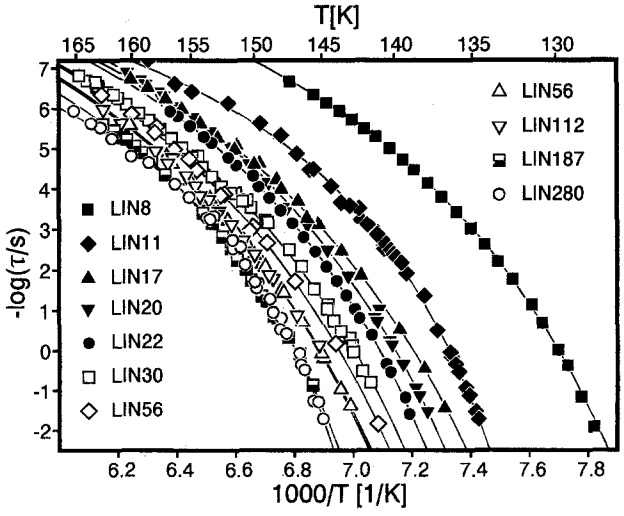

Fig. 3. Activation plot for linear PDMS samples. The lines are WLF-fits

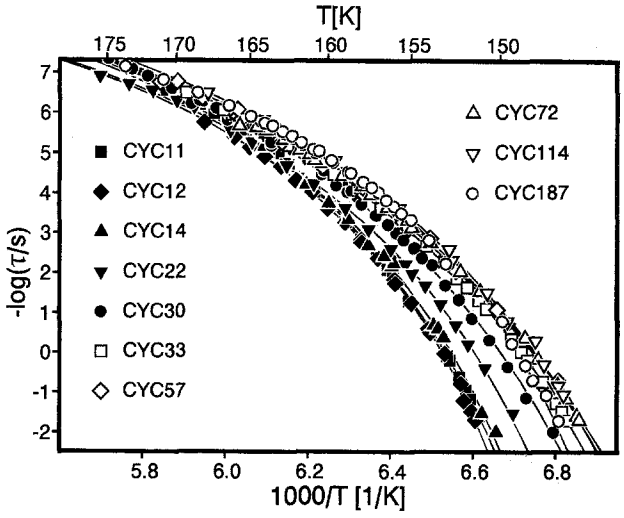

Fig. 4. Activation plot for cyclic samples with WLF-fits

Table 2. Havriliak–Negami-parameters of the α-relaxation of the sample LIN24 for different temperatures

T(K)	$\Delta\varepsilon$	α	γ	τ_{HN}
149.27	0.535	0.857	0.480	$3.41 \cdot 10$
150.82	0.535	0.849	0.485	2.49
151.76	0.535	0.877	0.452	$6.24 \cdot 10^{-1}$
152.44	0.535	0.862	0.451	$2.03 \cdot 10^{-1}$
153.29	0.527	0.845	0.445	$6.14 \cdot 10^{-2}$
154.17	0.520	0.852	0.476	$2.13 \cdot 10^{-2}$
155.35	0.520	0.860	0.468	$6.02 \cdot 10^{-3}$
156.19	0.504	0.839	0.466	$6.02 \cdot 10^{-3}$
157.54	0.517	0.845	0.450	$8.09 \cdot 10^{-4}$
158.93	0.488	0.888	0.448	$2.40 \cdot 10^{-4}$
160.86	0.484	0.863	0.466	$6.01 \cdot 10^{-5}$
162.58	0.471	0.876	0.461	$2.07 \cdot 10^{-5}$
164.85	0.462	0.876	0.460	$5.29 \cdot 10^{-6}$
166.28	0.441	0.866	0.472	$2.76 \cdot 10^{-6}$
168.76	0.401	0.847	0.484	$7.32 \cdot 10^{-7}$
169.97	0.331	0.851	0.486	$5.05 \cdot 10^{-7}$
171.66	0.250	0.872	0.465	$2.83 \cdot 10^{-7}$
173.35	0.161	0.871	0.464	$1.95 \cdot 10^{-7}$
175.49	0.094	0.876	0.486	$1.25 \cdot 10^{-7}$

Table 3. WLF fit parameters obtained with a reference relaxation time $\tau(T_s) = 1/\omega(T_s)$ of 1 s. C_1 and C_2 are WLF-fitparameters from which the free volume fraction $f = v_f/v = 1/[(\ln(10) \cdot C_1]$ and its thermal expansion coefficient $\alpha_f = 1/[(\ln(10) \cdot C_1 C_2]$ can be calculated

Sample	$\bar{n}$	$\frac{T_{g,\mathrm{DSC}}}{K}$	$\frac{T_s}{K}$	C_1	$\frac{C_2}{K}$	$\frac{v_f}{v} \cdot 100$	$\alpha_f \cdot 10^3\ \mathrm{K}$
LIN8	3	129.1	129.9	13.68	18.18	3.174	1.75
LIN11	4.5	135.9	136.5	11.46	14.01	3.789	2.7
LIN17	7.5	138.4	138.8	13.26	18.85	3.275	1.74
LIN20	9	140.3	139.9	13.8	22.26	3.146	1.41
LIN22	10	141.2	141.1	13.48	20.03	3.221	1.61
LIN24	11	143.6	141.3	14.11	22.34	3.077	1.38
LIN30	14	144.8	142.8	13.65	21.95	3.181	1.45
LIN56	27	147.5	143.8	14.32	23.37	3.032	1.3
LIN57	27.5	147.7	144.1	14.01	22.51	3.099	1.38
LIN86	42	148.8	145.3	14.12	23.06	3.075	1.33
LIN112	55	149.3	145.5	14.22	23.84	3.054	1.28
LIN187	92.5	149.4	147	12.59	19.15	3.449	1.8
LIN280	139	149.5	147	10.4	14.24	4.175	2.93
CYC8	4	–	–	–	–	–	–
CYC11	5.5	–	153	13.53	18.05	3.209	1.78
CYC12	6	–	153.2	11.49	14.55	3.779	2.6
CYC14	7	156.8	152.7	12.49	16.59	3.477	2.1
CYC22	11	154.9	150.8	12.03	17.27	3.609	2.09
CYC30	15	153.5	149.2	13.45	20.81	3.228	1.55
CYC33	16.5	152.5	148.8	13.1	20.86	3.315	1.59
CYC57	28.5	151.6	148.2	14.03	23.86	3.095	1.3
CYC72	36	150.9	148.2	12.72	20.4	3.414	1.67
CYC114	57	150.3	148.4	13.1	20.09	3.315	1.65
CYC115	57.5	150.3	148.5	12.73	20.05	3.411	1.7
CYC187	93.5	150.3	149	11.48	15	3.782	2.52

the calorimetric glass transition temperature $T_{g,\mathrm{DSC}}$ [24].

Besides the WLF-parameters and the temperatures T_s, Table 3 resembles the free volume fraction $f = (v_f/v)(T_s)$ and its thermal expansion coefficient α_f. For the sake of graphical resolution the WLF-temperatures T_s are plotted in Fig. 5 versus the logarithm of the number of repeat units. A representation of the data versus the inverse molecular weight is added in Fig. 6. The line fitting the data for linear samples obeys the Fox-Flory equation:

$$T_s = 147{,}0\ \mathrm{K} - \frac{5064\ \mathrm{g}}{M_n}\frac{K}{\mathrm{mol}}. \qquad (3.5)$$

After a slight minimum at CYC57 and CYC72, the temperature $T_s(n)$ for cyclic chains shows an increase with decreasing ring length and the hint of a maximum around n = 6. Generally, $T_{s,\mathrm{cyc}}(n)$

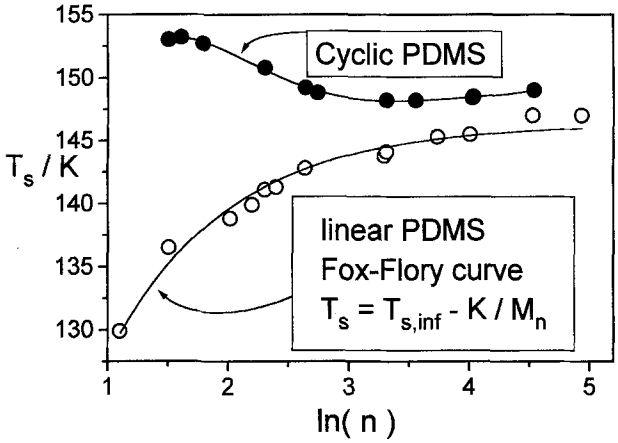

Fig. 5. The WLF-temperatures (with $\omega(T_s) = 1$ Hz) for linear (filled symbols) and cyclic PDMS (open symbols) vs. natural logarithm of the degree of polymerisation. The lower curve represents a Fox–Flory–fit, the upper one is a spline serving as guide for the eye

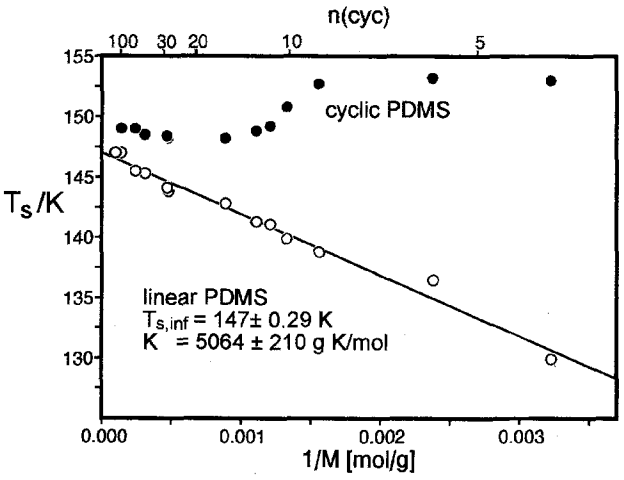

Fig. 6. The WLF-reference temperatures (wtih $\omega(T_s) = 1$ Hz) for linear (filled symbols) and cyclic PDMS (open symbols) vs. inverse molecular weight

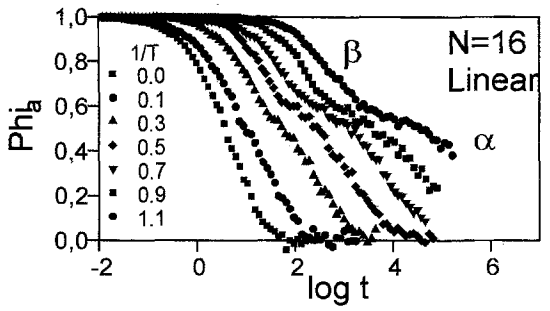

Fig. 7. Simulated autocorrelation-funtions of vectors representing a transversal dipole moment of linear chains having 16 bonds for several reduced temperatures

is higher than that of linear samples, as well as the free volume fraction f and its expansion coefficient. Variations of the latter are not observed due to the small temperature range.

4. Comparison with dynamic Monte–Carlo simulations

4.1 Simulations

Various molecular model systems with chains and rings comparable in length (N = 4, 8, 16, 32, 64) to the PDMS-samples under experimental investigation were generated on a lattice. The molecular dynamics of these systems were simulated by dynamic Monte–Carlo calculations. The applied algorithm uses dense systems in which the free volume fraction is not represented explicitly. Temperature and time are not determined on absolute scales They can be shifted by multiplication with some factors. In order to compare simulated and experimental results, a simulated activation curve must be shifted both in time and temperature and thus be fitted to experimental data. Henceforth, the relations between different simulated data and the shape of the activation curve have to be considered as the information obtained by the simulations.

The autocorrelation function of a dipole vector of a linear model chain of 16 repeat units is plotted for several temperatures in Fig. 7. Accor-

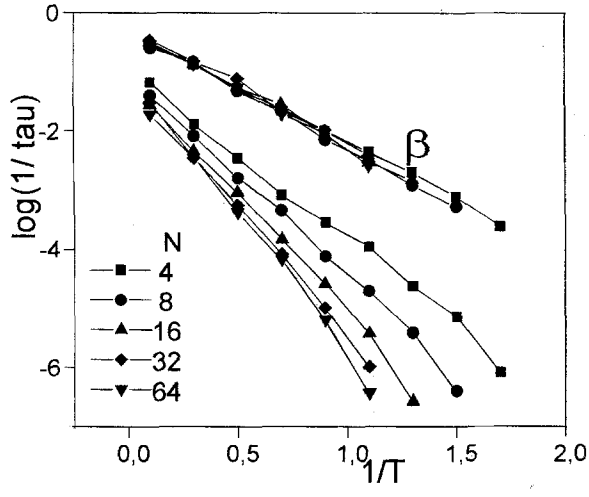

Fig. 8. Activation plot for the two relaxation components observed in simulations of linear chains with vaious lengths ($\tilde{T}$ is the reduced temperature and time is expressed by a number of Monte-Carlo steps per monomer)

ding to the simulations, this vector undergoes two relaxation processes, denoted with α and β. The β-process consists of local cooperative rearrangements appearing only in some places of the system with a suitable local configuration and does not lead to a global mobility. The global mobility, i.e., the α-process is achieved by a diffusive-like motion of the mobile areas throughout the whole system. The development of the two relaxation times with temperature is given in Fig. 8 for model systems of different chain length. The β-relaxation shows Arrhenius-behavior and is not dependent on chain length. In contrast, the activation curves of the α-relaxation are best and strongly dependent on the molecular mass.

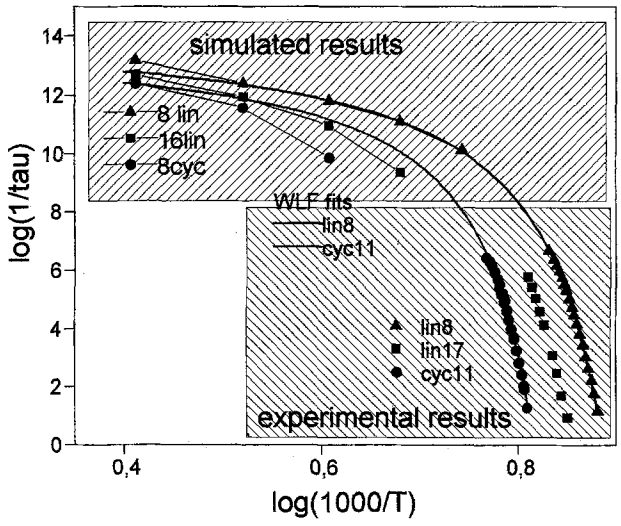

Fig. 9. Comparison of the simulated and experimental dielectric relaxation. The solid lines are WLF-fits to the experimental results. Bu multiplication of time and temperature with suitable factors ($\Delta\log(1/\tau)$ and $\Delta\log(1/T)$), the simulated data can be brought in good accordance with the experiments, e.g., for the chain with eight bonds (8 lin and LIN8, respectively)

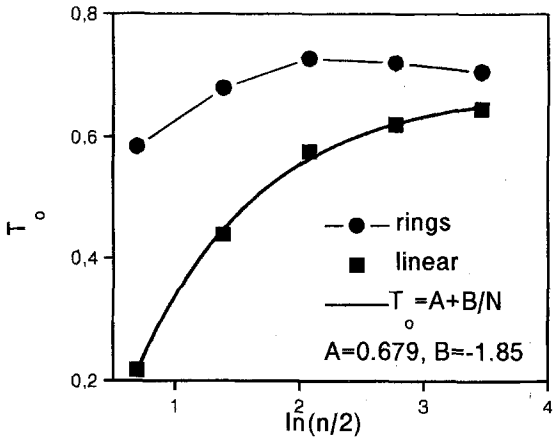

Fig. 10. The effect of the model chain length on a temperature T_0 defined by a reference frequency for the simulated relaxation. For linear chains a Fox–Flory-function is observed (solid line)

In Fig. 9 the simulated data is compared with the experimental results. By shifting the former in time and temperature as necessary with the applied simulation algorithm, good accordance is obtained, for example, for linear chains with eight bonds. The same shift results in stronger discrepancies for the cyclic pendants (sample CYC8 and simulation 8cyc). Obviously, the frequency range of the simulations and the dielectric experiments do not overlap due to limitations in calculation time. The spreading upward of the simulated WLF-curves is stronger than that of the experimentally determined curves.

In order to consider the molecular weight dependence of the simulated α-relaxation, Fig. 10 shows the temperature T_0 connected to a fixed reference relaxation time. The simulations result in a Fox–Flory-function for linear chains, whereas for rings they give a maximum in T_0 around $n = 8$.

Thus, the qualitative accordance of the simulations with experimental is astonishing. Discrepancies in detail may be due to two reasons: i) the model chain is an oversimplified picture of the real polymer chain, or ii) the temperature dependence of the free volume fraction is neglected in the simulations.

4.2 Discussion

There are two major observations which appear in former investigations of the glass transition temperature for linear and cyclic chains and which are reproduced in our results, as well: 1) for chains of the same length the glass transition for rings is always at higher temperatures than for linear chains, and 2) the chain length dependencies for the glass transition temperature for the two kinds converge to the same asymptotic value of T_g for long chains. These two major trends, which are found in a similar way for the activation energy E_{visc} of the bulk viscosity [9], the density and the refractive index of PMPS [6], are reproduced also in the simulation results reported in this paper and are predicted by the only theoretical treatment of this problem [7, 8], based on the considerations of differences in the configurational entropy between the two kinds of chains. This agreement, however only qualitative, suggests that the main effect in different behavior of rings and linear chains is caused by the fact that the configurational entropy of rings is generally much smaller than that of the linear chains. Qualitatively, the variation of the experimental glass transition temperature for both linear and cyclic chains is smaller than predicted by the theory or than observed in the simulation. Since the range of variation of T_g has been observed to be dependent on details of the chemical structure

of polymers, the discrepancies between experiments, on the one hand, and the theory or simulation, on the other hand, can be attributed to the fact that in both latter the structure of chains is oversimplified.

The results presented here have shown, however, that there are some features of behavior of ring which are not reflected even qualitatively in the theory considering only the configurational entropy of Gaussian chains. According to such theoretical treatment the glass transition for small rings should continuously shift to higher temperatures with decreasing length of chains. What we observe, both in the experimental and simulation results, is that there is a maximum in the chain length dependence appearing for rings consisting of several segments. This effect has also been observed in calorimetric DSC-T_g studies on poly(methyl-phenyl-siloxane)(PMPS) [11]. The fact that this effect is observed for different polymers as well as for the simplest chains considered in the simulation suggests its universality and the lack of this effect in theoretical predictions shows that there are some important factors in the considerations which are disregarded. This might be, for example, the deviations of rings in the melt from the Gaussian statistics, which was studied by Cates and Deutsch [32] and was demonstrated in the simulated melts of noncatenated rings [33]. Topological problems of packing of cyclic chains in such systems result in a scaling of ring dimensions with their polymerization degree ($R^2 \propto N^\nu$ with $\nu \approx 0.8$) which is intermediate between those for collapsed and Gaussian chains. This must remarkably affect the entropy of such systems and consequently influence the chain length dependence of the glass transition. There are certainly additional polymer specific effects, like, for example, chain stiffness or thermal expansion, which should be considered in the theory and in the simulation in order to attempt a quantitative description of the experimental results.

5. Conclusion

The dynamic glass transition (α-relaxation) of PDMS was studied in a 25 K wide temperature interval starting from $T_{g,\mathrm{DSC}}$ by dielectric spectroscopy. For this investigation samples of rings and linear chains of various molecular weight were used. The activation curves of this relaxation are in good accordance with the WLF-function. The dielectrically determined temperature $T_s = T(\tau = 1\ \mathrm{s})$ is up to 4 K beneath the DSC $- T_g$.

The relaxation rates and the values for T_s depend strongly on molecular structure and weight, whereas the shape of the relaxation time distribution seems not to be affected. While the relaxation of linear chains is shifted towards lower temperatures with decreasing molecular weight according to the Fox–Flory–equation, rings show the opposite trend having a maximum in T_s for rings of about six segments. Dynamic Monte–Carlo simulations of linear and cyclic model chains showed, besides a local Arrhenius-activated β-relaxation, an α-relaxation with WLF-type activation curves. The molecular weight dependence of this simulated α-relaxation is in a good qualitative agreement with the experimental observation for both linear and cyclic chains. Thus, the applied simulation method (CMA) has proven to be successful in the description of the molecular dynamics in dense polymeric systems.

Acknowledgement

The authors want to express their gratitude to J. Anthony Semlyen and Julien Hollingshurst (Department of Chemistry, University of York Heslington, York Y 01 5DD, UK) for kindly supplying the PDMS-samples.

References

1. Fox TG, Flory PJ (1950) J Appl Phys 21:581
2. Clarson SJ, Dodgson K, Semlyen JA (1985) Polymer 26:930
3. Dodgson K, Bannister DJ, Semlyen JA (1980) Polymer 21:633
4. Edwards CJC, Stepto RFT, Semlyen JA (1980) Polymer 21:781
5. Clarson SJ, Semlyen JA, Dodgson K (1991) Polymer 32:2823
6. Bannister DJ, Semlyen JA (1981) Polymer 22:377
7. DiMarzio EA, Guttman CM (1987) Macromolecules 20:1403
8. Yang AJ-M, DiMarzio EA (1991) Macromolecules 24:6012
9. Dodgson K, Bannister DJ, Semlyen JA (1980) Polymer 21:633
10. Edwards CJC, Stepto RFT, Semlyen JA (1980) Polymer 21:781
11. Clarson SJ, Semlyen JA, Dodgson K (1991) Polymer 32:2823

12. Hogen-Esch TE, Toreki W, Butler GB (1987) Polym Prepr (Am Chem Soc Div Polym Chem) 28:343 ibid (1989) 30:129
13. Pakula T (1987) Macromolecules 20:679
14. Dodgson K, Sympson D, Semlyen JA (1978) Polymer 19:1285
15. Semlyen JA, Wright PV (1977) In: Chromatography of Synthetic Polymers and Piopolymers (Ed. R. Epton), Ellis Horwood, Chichester
16. Adachi H, Adachi K, Ishida Y, Kotaka T (1979) J Polym Sci 17:851
17. Andrianov KA, Slonimskij GL, Zhdanov AA, Levin VYu, Levin Yu, Godovskij YuK, Moskalenko VA (1972) J Pol Sci Pol Chem Ed 10:1
18. Kremer F, Boese D, Meier G, Fischer EW (1980) Prog Coll Polym Sci 80:129
19. Havriliak S, Negami S (1966) J Polym Sci Part C 14:99
20. Havriliak S, Negami S (1967) Polymer 8:161
21. Mott NF, Davis EA (1979) Electronic Processes in non-crystalline Materials; Clarendon Press: Oxford, UK
22. Williams ML, Landel RF, Ferry JD (1955) J Am Chem Soc 77:3701
23. Ferry JD (1980) Viscoelastic properties of polymers, Wiley New York
24. Kirst KU, Kremer F, Litvinov VM (1993) Macromolecules 26:975
25. Fischer DJ (1961) J Appl Polym Sci 5:436
26. Lee CL, Johannson OK, Flaningam OL, Hahn P (1969) Polym Reprints Am Chem Soc 10, 1311.
27. Fröhlich H (1958) Theory of Dielectrics Oxford University Press, London
28. Böttcher CJF (1973) Theory of Electric Polarisation Elsevier Amsterdam
29. Ikada E, Fukushima H, Watanabe T (1979) J Polym Sci Polym Phys 17:1789
30. Beevers MS, Mumby SJ, Clarson SJ, Semlyen JA (1983) Polymer 24:1564
31. Hofmann A (1993) Thesis, University of Mainz
32. Cates ME, Deutsch JM (1986) J Physique 47:2121
33. Pakula T, Edling T (1990) in Basic Feature of the Glass Transition; Eds.: Colmenero, J Alegria A World Scientific New Jersey 1990, 235.
34. Pakula T, Geyler S (1987) Macromolecules 20:2909
35. Pakula T, Geyler S (1988) Macromolecules 21:1665
36. Geyler S, Pakula T (1988) Macromol Chem 9:617
37. Reiter J, Geyler S, Pakula T (1990) J Chem Phys 93:837
38. Pakula T (in preparation)

Received May 13, 1994;
accepted June 27, 1994

Authors' address:

Dr. K. Ulrich Kirst
Institut für Physik
Universität Leipzig
Linnéstraße 5
04103 Leipzig, FRG